Investigation of the Electromagnetic Structure of η and η' Mesons by Two-Photon Interactions

H. Aihara, M. Alston-Garnjost, R. E. Avery, A. Barbaro-Galtieri, A. R. Barker, B. A. Barnett, D. A. Bauer, A. Bay, G. J. Bobbink, C. D. Buchanan, A. Buijs, D. O. Caldwell, H-Y. Chao, S-B. Chun, A. R. Clark, G. D. Cowan, D. A. Crane, O. I. Dahl, M. Daoudi, K. A. Derby, J. J. Eastman, P. H. Eberhard, T. K. Edberg, A. M. Eisner, F. C. Erné, K. H. Fairfield, J. M. Hauptman, W. Hofmann, J. Hylen, T. Kamae, H. S. Kaye, R. W. Kenney, S. Khacheryan, R. R. Kofler, W. G. J. Langeveld, J. G. Layter, W. T. Lin, F. L. Linde, S. C. Loken, A. Lu, G. R. Lynch, R. J. Madaras, B. D. Magnuson, G. E. Masek, L. G. Mathis, J. A. J. Matthews, S. J. Maxfield, E. S. Miller, W. Moses, D. R. Nygren, P. J. Oddone, H. P. Paar, S. K. Park, D. E. Pellett, M. Pripstein, M. T. Ronan, R. R. Ross, F. R. Rouse, K. A. Schwitkis, J. C. Sens, G. Shapiro, B. C. Shen, J. R. Smith, J. S. Steinman, R. W. Stephens, M. L. Stevenson, D. H. Stork, M. G. Strauss, M. K. Sullivan, T. Takahashi, S. Toutounchi, R. van Tyen, W. Vernon, W. Wagner, E. M. Wang, Y-X. Wang, W. A. Wenzel, Z. R. Wolf, H. Yamamoto, S. J. Yellin, and C. Zeitlin

(TPC/Two-Gamma Collaboration)

Lawrence Berkeley Laboratory, University of California, Berkeley, California 94720
University of California, Davis, California 95616
University of California Intercampus Institute for Research at Particle Accelerators, Stanford, California 94305
University of California, Los Angeles, California 90024
University of California, Riverside, California 92521
University of California, San Diego, California 92093
University of California, Santa Barbara, California 93106
Ames Laboratory, Iowa State University, Ames, Iowa 50011
Johns Hopkins University, Baltimore, Maryland 21218
University of Massachusetts, Amherst, Massachusetts 01003
National Institute for Nuclear and High Energy Physics, Amsterdam, The Netherlands
University of Tokyo, Tokyo, Japan
(Received 21 August 1989)

The TPC/Two-Gamma facility at the SLAC e^+e^- storage ring PEP was used to study the reactions $\gamma\gamma^* \to \eta$ and $\gamma\gamma^* \to \eta'$. The $\eta\gamma^*\gamma$ and $\eta'\gamma^*\gamma$ transition form factors were measured as functions of Q^2, the negative of the invariant mass squared of the tagged photon, in the range $0.1 < Q^2 < 7$ GeV^2. These determinations of the electromagnetic structure of the η and η' mesons are consistent with both vector-meson dominance and QCD. They also provide new measurements of the pseudoscalar mixing angle and decay constants.

PACS numbers: 13.40.Fn, 12.38.Qk, 12.40.Vv, 14.40.Cs

The formation of mesons in two-photon reactions provides information on their electromagnetic structure. While production by two nearly real photons measures quark charges, production involving one quite virtual photon also tests QCD. The light pseudoscalar mesons may provide a particularly sensitive testing ground, since for massless u, d, and s quarks the pseudoscalar mesons would consist of a massless octet of Goldstone bosons plus a massive SU(3) singlet. With nonzero quark masses, the physical eigenstates are given by $\eta = \eta_8 \cos\theta_P - \eta_1 \sin\theta_P$ and $\eta' = \eta_8 \sin\theta_P + \eta_1 \cos\theta_P$, where the pseudoscalar mixing angle $\theta_P \approx -20°$.[1] Nonperturbative QCD calculations involving chiral symmetry, the triangle anomaly, and the Wess-Zumino-Witten Lagrangian have successfully described the pseudoscalar-meson couplings to real photons.[2] It has recently been pointed out[3,4] that higher-order chiral contributions can be studied if one photon is virtual, even with small values of Q^2, the negative of the invariant mass squared of the virtual photon. At large Q^2, where QCD perturbation theory should apply, the leading-order predictions of Brodsky and Lepage[5] provide a framework for interpreting the Q^2 dependence of the pseudoscalar transition form factors.

Reported here is the first determination of the $\eta\gamma^*\gamma$ transition form factor by two-photon production, along with a new measurement of the $\eta'\gamma^*\gamma$ form factor, for which there have been several previous results.[6-9] These pseudoscalar mesons (P) were produced in the reaction $e^+e^- \to e^+e^-\gamma\gamma^* \to e^+e^-P$, where the detection of either the e^+ or e^- tagged the virtual photon (γ^*). The η and η' were then observed in the final-state $\pi^+\pi^-\gamma$ via direct decays and also via decay chains with one additional, undetected, photon. The data were collected with

the TPC/Two-Gamma facility at the SLAC storage ring PEP. The integrated luminosity was 113 pb^{-1} at an e^+e^- center-of-mass energy of 29 GeV.

The TPC/Two-Gamma facility has been described elsewhere,[10] but features relevant to this analysis are mentioned here. The Time Projection Chamber (TPC) was used to separate pions from electrons, kaons, and protons by simultaneous measurements of momentum p and energy loss dE/dx. The TPC magnetic field was 4 kG for the first 50 pb^{-1} of data, and the typical momentum resolution was $\sigma/p \approx 6\%$. For the remaining 63 pb^{-1} of data, the magnetic field was 13 kG and there was less material in front of the TPC, giving an improved momentum resolution of $\sigma/p \approx 1.5\%$. The dE/dx determination had a typical resolution of 3.5%. Two pole-tip calorimeters (PTC) and a hexagonal barrel calorimeter (HEX) provided electromagnetic shower detection for polar angles above 260 mrad. There were cylindrical drift chambers at the inner and outer radii of the TPC. Particles were also detected in the forward-backward directions at polar angles between 25 and 180 mrad. Charged particles in these regions were tracked by spectrometers, each containing fifteen drift-chamber planes and a septum magnet. Electromagnetic calorimetry was also provided at small angles by arrays of NaI crystals (25–90 mrad) and Pb-scintillator shower counters (100–180 mrad).

In the analysis, events were selected with two oppositely charged particles, one photon, and a scattered e^+ or e^- (a "tag"). The tag was required to have a charged track in the forward drift chambers pointing to an energy deposition greater than 5 GeV in the NaI or greater than 10 GeV in the lead-scintillator detector. At least one charged particle had to be in the TPC fiducial volume, and any track there was required to be identified as a pion (or muon) by dE/dx and to extrapolate to within 5 cm of the interaction point along the beam line. Final-state photons were required to have measured energies of at least 70 MeV in the HEX, or 100 MeV in the PTC. Background from nonexclusive events was suppressed by requiring missing $p_\perp < 0.6$ GeV and $|\cos\theta^*| < 0.75$, where θ^* is the angle between the final-state γ and the π^+ in the $\pi^+\pi^-$ center-of-mass frame.[11] The angle cut also suppressed backgrounds from bremsstrahlung-type radiative corrections to $e^+e^- \to e^+e^-\mu^+\mu^-$ or $e^+e^- \to e^+e^-\pi\pi$ processes. Events with identified photons in the NaI or lead-scintillator detector were eliminated, further suppressing radiative backgrounds.

Events passing these cuts were kinematically fitted to an $e^+e^-\pi^+\pi^-\gamma$ final state[12] and were kept if they had a confidence level for the fit of at least 5% and a fitted photon energy > 100 MeV. Figure 1 shows the $\pi^+\pi^-\gamma$ invariant-mass spectrum for the 540 events remaining in the data. A clear $\eta'(958)$ signal is seen, along with two other peaks which we ascribe to the $\eta(549)$ and the

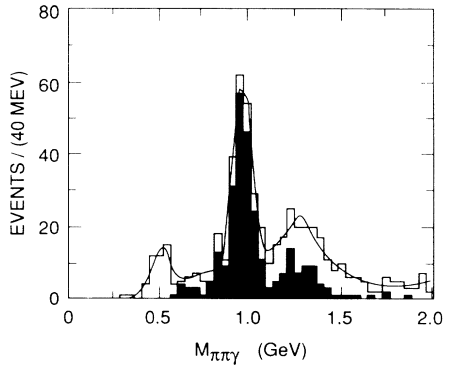

FIG. 1. $\pi^+\pi^-\gamma$ mass spectra as determined from kinematically fitted quantities. The shaded histogram is the $\pi^+\pi^-\gamma$ invariant-mass spectrum for those events with a $\pi^+\pi^-$ invariant mass in the ρ^0 region, between 500 and 850 MeV. The curve is the best fit to the whole sample, as described in the text.

$a_2(1320)$. The latter two resonances appear in this spectrum due to their decays $\eta \to \pi^+\pi^-\pi^0$ (with branching ratio $B = 23.7\%$) and $a_2^0 \to \rho^\pm\pi^\mp \to \pi^+\pi^-\pi^0$ ($B = 70.1\%$), coupled in each case with the nonobservance of one π^0-decay photon, as well as the direct decay $\eta \to \pi^+\pi^-\gamma$ ($B = 4.9\%$).[13] The η' signal comes from the decay $\eta' \to \rho^0\gamma$, $\rho^0 \to \pi^+\pi^-$ ($B = 30.1\%$) and from the decay $\eta' \to \pi^+\pi^-\eta$, $\eta \to \gamma\gamma$ ($B = 17.2\%$).[14] If we require the $\pi^+\pi^-$ invariant mass to be in the ρ^0 region, between 500 and 850 MeV, the shaded histogram in Fig. 1 results.

To determine the acceptance, events were generated in a Monte Carlo program based on the $\gamma\gamma$ luminosity function of Ref. 15 and on the matrix element $i\sqrt{X}F_{P\gamma}(q_1^2,q_2^2)$ defined in Ref. 16 for the production of a narrow pseudoscalar resonance P by two virtual photons. Here $F_{P\gamma}$ is the form factor and $X \equiv (q_1\cdot q_2)^2 - q_1^2q_2^2$, with q_i the photon four-momenta. The two-photon decay width is then given by

$$\Gamma_{P\to\gamma\gamma} = (m_P^3/64\pi)F_{P\gamma}^2(0,0)\,. \tag{1}$$

The cross section for $\gamma^*\gamma^* \to P$ is

$$\sigma_{\gamma^*\gamma^*\to P} = \frac{\pi}{4}\sqrt{X}F_{P\gamma}^2(q_1^2,q_2^2)\delta(W^2 - m_P^2)\,, \tag{2}$$

where $W^2 \equiv (q_1+q_2)^2$, the $\gamma^*\gamma^*$ invariant mass squared. For the q^2 dependence of $F_{P\gamma}$, the Monte Carlo simulation used a factorized form suggested by vector-meson (ρ) dominance,

$$F_{P\gamma}^2(q_1^2,q_2^2) = \frac{64\pi\Gamma_{P\to\gamma\gamma}}{m_P^3} \times \left(\frac{1}{1-q_1^2/m_\rho^2}\right)^2\left(\frac{1}{1-q_2^2/m_\rho^2}\right)^2. \tag{3}$$

Note that, in our single-tagged measurement, one of the

virtual photons is nearly real ($q_i^2 \approx 0$) and the other has $Q^2 = -q^2 > 0.1$ GeV^2. The decays $\eta' \to \rho^0\gamma \to \pi^+\pi^-\gamma$ and $a_2^0 \to \rho^\pm\pi^\mp \to \pi^+\pi^-\pi^0$ were simulated in the same manner as in our previous publication,[6,17] while the η meson decays into $\pi^+\pi^-\gamma$ and $\pi^+\pi^-\pi^0$ and the η' decay into $\pi^+\pi^-\eta \to \pi^+\pi^-\gamma\gamma$ were simulated according to three-particle phase space.[18] The generated events were subjected to a detector simulation which included effects of nuclear interactions, energy loss and multiple scattering in the detector materials, decays of the final-state particles, detector response, triggering, the kinematic fit, and the experimental cuts.

The data sample is fit well by a sum of an η' Gaussian,[19] η and a_2^0 Monte Carlo shapes, and a third-degree polynomial to account for any nonresonant background,[17] as shown in Fig. 1. Since there is less background underneath the η' meson for those events with a ρ^0, we used the $\pi^+\pi^-\gamma$ spectrum with the ρ^0 requirement when estimating the number of η' mesons in the data. The fits gave 38.0 ± 9.4 η mesons and 159.2 ± 14.7 η' mesons. The events were then separated into five Q^2 bins and, from the $\pi^+\pi^-\gamma$ invariant-mass spectrum in each Q^2 bin, the η and η' content were determined as above. Figure 2 shows the measured values of $m_P^3 F_{P\gamma}^2/64\pi$ as a function of Q^2 for the η and η' mesons. Not shown in this figure is the 12% systematic error in both the η and η' measurements which arises from uncertainties in the background shape for the η (8%) and the η' (6%), integrated luminosity (6%), knowledge of the η and η' acceptances (7% and 6%, respectively), and the values of the various branching fractions for the η and η' (2% and 5%, respectively).

According to the Brodsky-Lepage QCD calculation[5] $F_{P\gamma} \to 8\pi\alpha f_P/Q^2$ as $Q^2 \to \infty$, where f_P is the decay constant for the pseudoscalar P. Furthermore, current algebra gives $F_{P\gamma} \to \alpha/\pi f_P$ as $Q^2 \to 0$. One can then write a reasonable interpolation form between these quite separate QCD predictions:[5]

$$F_{P\gamma}(Q^2) = \frac{\alpha}{\pi f_P} \frac{1}{1 + Q^2/8\pi^2 f_P^2} . \tag{4}$$

As a test of this QCD-inspired form, we fit the measured values of $m_P^3 F_{P\gamma}^2(Q^2)/64\pi$, together with world averages for the $Q^2 = 0$ points,[20] using the form

$$F_{P\gamma}(Q^2) = \frac{A}{1 + (Q^2/\Lambda_P^2)^n} . \tag{5}$$

This fit yields the values $n - 1 = 0.08 \pm 0.15$ for the η' and $n - 1 = 0.09 \pm 0.29$ for the η, both of which are clearly consistent with the $1/Q^2$ dependence predicted by QCD at large Q^2.

Fixing $n = 1$, the fits then yield values for the characteristic masses $\Lambda_\eta = 0.70 \pm 0.08$ GeV and $\Lambda_{\eta'} = 0.85 \pm 0.07$ GeV. Using the decay $\eta \to \mu^+\mu^-\gamma$, the Lepton-$G$ experiment[21] obtained the result $\Lambda_\eta = 0.72 \pm 0.09$ GeV, which is in good agreement with our value.

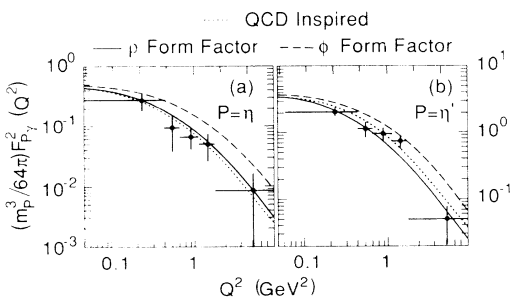

FIG. 2. $m_P^3 F_{P\gamma}^2/64\pi$ as a function of Q^2 for the (a) η meson and (b) η' meson. The horizontal error bars denote the limits of the Q^2 bins, with the points plotted at the center of the bins. The vertical error bars indicate the 65% confidence limits based upon Gaussian statistical errors only. The curves shown are from the QCD-inspired model described in the text as well as the predictions of VMD.

Quark-loop calculations[4,22] predict $\Lambda_\eta = 0.72$ GeV and $\Lambda_{\eta'} = 0.85$ GeV, also in good agreement with our measurements. The curves described as "QCD inspired" in Fig. 2, which fit the data well, were obtained using (5) with $n = 1$ and the quark-loop values for Λ_P, together with the normalizations provided by world-average values for $\Gamma_{P\gamma\gamma}$. Figure 2 also shows the predictions of vector-meson dominance (VMD) normalized in the same manner. The ρ form factor provides a good fit for the η and the ϕ form factor does not; the situation is less clear for the η'. Unfortunately, differences between VMD predictions and the QCD-inspired interpolation form factors are too small to be distinguished by present data.

The weak decay constants f_η and f_η' can also be determined from the data. Comparing the Q^2 dependence from (4) and (5) gives $f_\eta = 79 \pm 9$ MeV and $f_\eta' = 96 \pm 8$ MeV, both similar to $f_\pi = 93$ MeV determined from leptonic decays. However, since the normalization in (5) is determined mainly by the well-known two-photon widths of the pseudoscalar mesons, the comparison with the normalization of (4) can give more precise results for the decay constants. The resulting values $f_\eta = 91 \pm 6$ MeV and $f_\eta' = 78 \pm 5$ MeV, are in reasonable agreement with the values derived from the Q^2 dependence along, thus lending credibility to the QCD-inspired interpolation formula (4).

Chiral-symmetry calculations have predicted[2,23] the octet decay constant $f_8 \approx 1.25 f_\pi$. Using this value and the relations

$$\frac{1}{f_\eta} = \frac{1}{\sqrt{3}} \left(\frac{\cos\theta_P}{f_8} - \frac{\sqrt{8}\sin\theta_P}{f_1} \right) , \tag{6}$$

$$\frac{1}{f_\eta'} = \frac{1}{\sqrt{3}} \left(\frac{\sin\theta_P}{f_8} + \frac{\sqrt{8}\cos\theta_P}{f_1} \right) , \tag{7}$$

we can derive measurements of the pseudoscalar mixing angle and the singlet decay constant f_1 from the values

for f_η and $f_{\eta'}$. The Q^2 dependence alone gives $f_1 = (1.12 \pm 0.12) f_\pi$ and $\theta_P = -33° \pm 8°$, where the errors are statistical only. Using instead the normalizations determined mainly by two-photon widths leads to $f_1 = (1.09 \pm 0.08) f_\pi$ and $\theta_P = -23° \pm 8°$.

In conclusion, we have made the first measurement of the $\eta\gamma^*\gamma$ form factor using two-photon interactions, as well as making an improved measurement of the $\eta'\gamma^*\gamma$ form factor. The Q^2 dependence of these form factors is consistent with vector-dominance predictions but also with the power-law behavior expected from QCD at high Q^2. Even in the limited Q^2 range available here, the data are useful for extracting parameters of interest in QCD.

We gratefully acknowledge the efforts of the PEP staff and the engineers, programmers, and technicians of the collaborating institutions. We also wish to thank S. J. Brodsky and J. F. Donoghue for many useful discussions. This work was supported in part by the U.S. Department of Energy, the National Science Foundation, the Joint Japan–U.S. Collaboration in High Energy Physics, and the Foundation for Fundamental Research on Matter in The Netherlands.

[1]F. J. Gilman and R. Kauffman, Phys. Rev. D **36**, 2761 (1987).

[2]J. F. Donoghue, B. R. Holstein, and Y. Lin, Phys. Rev. Lett. **55**, 2766 (1985).

[3]J. F. Donoghue and D. Wyler, University of Massachusetts Report No. UMHEP-312, 1988 (to be published); Nucl. Phys. B (to be published).

[4]J. Bijnens, A. Bramon, and F. Cornet, Phys. Rev. Lett. **61**, 1453 (1988).

[5]S. J. Brodsky and G. P. Lepage, Phys. Rev. D **24**, 1808 (1981); note that there is a factor of $4\pi\alpha$ difference in convention for the definition of form factors between this reference and our analysis.

[6]H. Aihara *et al.*, Phys. Rev. D **35**, 2650 (1987); this previous measurement of the $\eta'\gamma^*\gamma$ form factor used only a 50-pb^{-1} subset of the present sample.

[7]Ch. Berger *et al.*, Phys. Lett. **142B**, 125 (1984).

[8]H. Aihara *et al.*, Phys. Rev. D **38**, 1 (1988).

[9]G. Gidal *et al.*, Phys. Rev. Lett. **59**, 2012 (1987).

[10]H. Aihara *et al.*, Lawrence Berkely Laboratory Report No. LBL 23737 (to be published).

[11]These cuts are a compromise between rejecting undesired and nonexclusive background and keeping the events from decay chains where one of the final-state photons is undetected. We rely on Monte Carlo calculations to simulate the effect of the cuts on these latter reactions.

[12]The untagged e^+ or e^- is constrained in the fit to lie within 3.4 mrad of the beam axis, a region where the fitting efficiency is large and well understood. We have corrected for the small ($< 10\%$) number of tagged η and η' events which the Monte Carlo simulation predicts will fail to fit due to this requirement.

[13]Monte Carlo simulations predict that 23% of our η mesons come from the direct decay $\eta \to \pi^+\pi^-\gamma$.

[14]Monte Carlo simulations predict that 7% of our η' mesons come from the decay into $\pi^+\pi^-\eta$.

[15]V. E. Balakin, V. M. Budnev, and I. F. Ginzburg, Pis'ma Zh. Eksp. Teor. Fiz. **11**, 559 (1970) [JETP Lett. **11**, 388 (1970)]; G. Bonneau, M. Gourdin, and F. Martin, Nucl. Phys. **B54**, 573 (1973); V. M. Budnev *et al.*, Phys. Rep. **15C**, 181 (1975).

[16]G. Köpp, T. F. Walsh, and P. Zerwas, Nucl. Phys. **B70**, 461 (1974).

[17]Kent Schwitkis, Ph.D. thesis, University of California, Santa Barbara, 1987 (unpublished).

[18]A Rittenberg, Ph.D. thesis, University of California, Berkeley, University of California Report No. UCRL-18863, 1969 (unpublished); J. G. Layter *et al.*, Phys. Rev. D **7**, 2565 (1973).

[19]The Gaussian shape gives a slightly better fit for the η' than does the Monte Carlo distribution, presumably due to difficulties in simulating the decay via the very broad ρ^0. The difference in estimated numbers of events between the two methods has been included in the systematic error estimates for our results.

[20]We have calculated these world averages ($\Gamma_{\eta \to \gamma\gamma} = 0.54 \pm 0.05$ keV and $\Gamma_{\eta' \to \gamma\gamma} = 4.13 \pm 0.31$ keV) using only recent, published, two-photon experimental results.

[21]R. I. Djhelyadin *et al.*, Phys. Lett. **94B**, 548 (1980). This reference gives the results of earlier experiments using the decay $\eta \to e^+e^-\gamma$, which have large errors and require large radiative corrections.

[22]A. Bramon and E. Masso, Phys. Lett. **104B**, 311 (1981).

[23]J. Gasser and H. Leutwyler, Nucl. Phys. **B250**, 465 (1985).

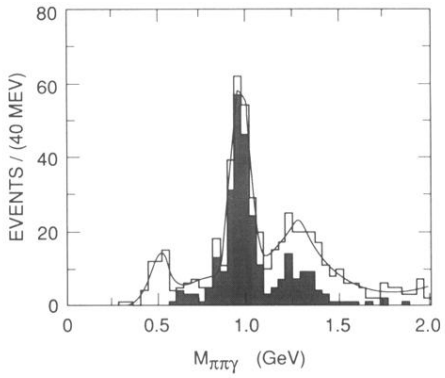

FIG. 1. $\pi^+\pi^-\gamma$ mass spectra as determined from kinematically fitted quantities. The shaded histogram is the $\pi^+\pi^-\gamma$ invariant-mass spectrum for those events with a $\pi^+\pi^-$ invariant mass in the ρ^0 region, between 500 and 850 MeV. The curve is the best fit to the whole sample, as described in the text.